

# Hydrodeoxygenation of Anisole via Cu supported on Zeolite: HZSM-5, MOR, and Indonesian Activated Natural Zeolite

## Hidrodesoxigenación de anisol mediante Cu soportado en zeolita: HZSM-5, MOR y zeolita natural activada de Indonesia

Khoirina Dwi Nugrahaningtyas<sup>1</sup>, Aji Indo Sabiilagusti<sup>2</sup>, Fitria Rahmawati<sup>3</sup>, Eddy Heraldry<sup>4</sup>, and Yuniawan Hidayat<sup>5</sup>

### ABSTRACT

The conversion of biomass waste into an alternative energy source requires effective and efficient hydrodeoxygenation (HDO) catalysts. This research aimed to synthesize a bifunctional zeolite-based catalyst for anisole conversion into BTX. The noble metal Cu was impregnated on HZSM-5, mordenite, and Indonesian activated natural zeolite (ANZ) to form HDO catalysts. X-ray fluorescence (XRF), X-ray diffraction (XRD), surface area and pore profile analysis, Fourier transform infrared analysis, ammonia-temperature programmed desorption (NH<sub>3</sub>-TPD), pyridine gravimetry, morphology, and scanning electron microscopy-energy dispersion elemental mapping (SEM-EDX) were used to determine the catalyst's properties. The HDO reaction test used anisole as a model compound in a semi-flow reactor with hydrogen gas at 350 and 500 °C for 1 h. Copper nanocrystals were found on the surface of the zeolites in several metal phase types, including Cu, Cu<sub>2</sub>O, CuO, and Cu(OH)<sub>2</sub>. Due to the copper bonds inside the zeolite pores, the internal pore surface area decreased. The acidity also decreased since it is strongly related to the surface area. At 350 °C, Cu was found to be less active. However, at 500 °C, copper activity increased, leading to an increase in anisole conversion and BTX selectivity. The catalyst with the highest anisole conversion and BTX selectivity was Cu/HZSM-5 (i.e., 53,28 and 13,06% v, respectively).

**Keywords:** acidity, BTX, copper, metal phase, surface area

### RESUMEN

La conversión de residuos de biomasa en una fuente de energía alternativa requiere catalizadores de hidrodesoxigenación (HDO) efectivos y eficientes. Esta investigación tuvo como objetivo sintetizar un catalizador bifuncional a base de zeolita para la conversión de anisol en BTX. El metal noble Cu se impregnó en HZSM-5, mordenita y zeolita natural activada de Indonesia (ANZ) para formar catalizadores HDO. Se empleó fluorescencia de rayos X (XRF), difracción de rayos X (XRD), análisis de área superficial y del perfil de los poros, análisis infrarrojo por transformada de Fourier, desorción programada a temperatura de amoníaco (NH<sub>3</sub>-TPD), gravimetría de piridina, morfología y mapeo elemental de dispersión de energía por microscopía electrónica de barrido (SEM-EDX) para determinar las propiedades del catalizador. La prueba de reacción HDO utilizó anisol como compuesto modelo en un reactor de semiflujo con gas hidrógeno a 350 y 500 °C durante 1 h. Se encontraron nanocristales de cobre en la superficie de las zeolitas en varios tipos de fases metálicas, incluyendo Cu, Cu<sub>2</sub>O, CuO y Cu(OH)<sub>2</sub>. Debido a los enlaces de cobre dentro de los poros de la zeolita, el área de la superficie del poro interno disminuyó. La acidez también se redujo, pues está estrechamente relacionada con la superficie. A 350 °C, se encontró que el Cu era menos activo. Sin embargo, a 500 °C, la actividad del cobre aumentó, lo que provocó un aumento en la conversión de anisol y la selectividad de BTX. El catalizador con la mayor conversión de anisol y selectividad de BTX fue Cu/HZSM-5 (i.e., 53,28 y 13,06 % v respectivamente).

**Palabras clave:** acidez, BTX, cobre, fase metálica, área superficial

**Received:** January 10<sup>th</sup>, 2023

**Accepted:** July 28<sup>th</sup>, 2023

<sup>1</sup> Chemistry Department, Universitas Gadjah Mada, Indonesia. Dr., Universitas Gadjah Mada, Indonesia. Affiliation: Full professor, Sebelas Maret University, Indonesia. E-mail: khoirinadwi@staff.uns.ac.id

<sup>2</sup> Chemistry Department, Sebelas Maret University, Indonesia. M.Si-c Sebelas Maret University, Indonesia. Affiliation: Master student, Sebelas Maret University, Indonesia. E-mail: aji.sabiila@student.uns.ac.id

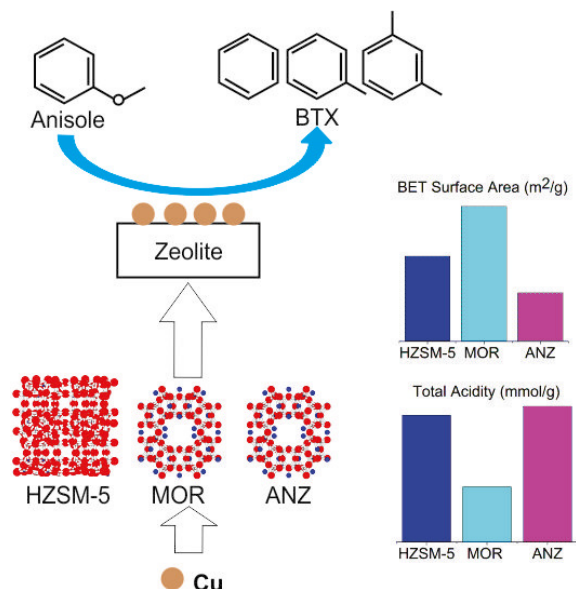
<sup>3</sup> Chemistry Department, Universitas Brawijaya, Indonesia. M.Si, Universitas Gadjah Mada, Indonesia. Dr, Institut Teknologi Bandung, Indonesia. Affiliation: Full Professor, Sebelas Maret University, Indonesia. E-mail: fitria@mipa.uns.ac.id

<sup>4</sup> Chemistry Department, Universitas Gadjah Mada, Indonesia. Dr., Universitas Gadjah Mada, Indonesia. Affiliation: Full professor, Sebelas Maret University, Indonesia. E-mail: eheraldy@mipa.uns.ac.id

<sup>5</sup> Chemistry Department, Universitas Gadjah Mada, Indonesia. Dr., Universitas Gadjah Mada, Indonesia. Affiliation: Associate professor, Sebelas Maret University, Indonesia. E-mail: yuniawan.hidayat@mipa.uns.ac.id



## Graphical abstract



## Introduction

Biomass-based fuels have been extensively studied to solve supply shortages and environmental issues [1], [2]. Non-edible sources such as lignin may be a promising option for overcoming this issue, as it is easily found in many types of wood, including cheap wood and paper industry waste [3], [4]. The main liquid output of rapid lignin pyrolysis is bio-oil. This product has a low calorific value and is corrosive, so it cannot directly replace petroleum [5]. Therefore, catalytic hydrodeoxygenation (HDO) is required to remove the oxygen content from pyrolysis products in order to meet the requirements for transportation fuels or those for conventional fossil fuel additives. Fast pyrolysis followed by HDO is the preferred method for converting lignin to aromatic hydrocarbons as fuel fractions, such as benzene, toluene, and xylene (BTX) [1], [6], [7].

Transition metal-supported catalysts have excellent performance in the HDO of biomass-derived oils to produce aromatic hydrocarbons [2], [5]. However, Cu-supported catalysts for HDO have not received much attention [4], [8]. This is intriguing because Cu has good adsorption capabilities as per the Sabatier principle, which are almost equal to those of noble metals such as Pt, Pd, and Ru [9]. By comparing it to Ni, Co, and Mo, [4] discovered that Cu-supported HZSM-5 has the highest liquid product in the HDO of anisole, a model compound of lignin-derived oil. [8] found that depositing Cu into the pores of ZSM-5 gradually reduced the surface area of the catalyst. Surprisingly, a 5% (w/w) Cu loading increased the acidity of ZSM-5, but an excessive increase in the Cu concentration (above 10% w/w) dramatically reduced the acidity and the catalyst activity.

Supports for HDO have been extensively researched, including inert materials (such as SiO<sub>2</sub> and Al<sub>2</sub>O<sub>3</sub>), activated

carbon, metal oxides, and acid materials such as zeolite. Zeolite is the most promising of these materials due to its high thermal stability, shape selectivity, and adjustable acidity [4]. Because of its high acidity and small pore size, HZSM-5 has a high selectivity for converting oxygenated compounds to aromatic hydrocarbons [10]-[12]. However, HZSM-5 has a hard time in converting large oxygenated compounds [13], and excessive metal concentrations easily block its pores [8]. Studying ideal supports or identifying alternate supports with wide pores is a challenging task. Therefore, this study was dedicated to synthesizing and comparing HDO catalyst-based copper with various carriers (*i.e.*, HZSM-5, MOR, and ANZ).

## Experimentation

### Materials

The support materials used for catalyst synthesis were HZSM-5 (SiO<sub>2</sub>/Al<sub>2</sub>O<sub>3</sub> = 26) supplied by ACS Material, H-Mordenite HS-690 (SiO<sub>2</sub>/Al<sub>2</sub>O<sub>3</sub> = 200, MOR) supplied by Wako Chemical USA, and Indonesian Natural zeolite (NZ).

### Synthesizing Cu-supported zeolite

We produced Indonesian-activated natural zeolite (ANZ) while following our prior studies [14], [15]. The bi-functional catalysts were produced using wet impregnation. Several zeolites, ammonia, and Cu(NO<sub>3</sub>)<sub>2</sub>·3H<sub>2</sub>O (p.a, E Merck) were blended and then refluxed for 16 hours at 30 °C and then at 80 °C for 4 hours [16], [17]. Then, the impregnated zeolite was dried in a rotary evaporator (IKA RV 05 Basic) at a pressure of 72 mBar and at 40 °C. The dry powder was then calcined for 3 hours at 550 °C in N<sub>2</sub> gas and then reduced for 2 hours at 400 °C in H<sub>2</sub> gas. The catalysts were labeled

as  $Cu_x/Z$ , where  $x$  represents the concentration of Cu (0, 4, or 8) and  $Z$  denotes the zeolite (HZSM-5, MOR, or ANZ).

### Characterization

Except for MOR, which involved a BRUKER S2 Ranger, the elemental composition of the catalyst was determined using PANalytical's Minipal 4 X-ray fluorescence (XRF) instrument. Simultaneously, X-ray diffraction spectroscopy (XRD, Rigaku Miniflex) was used to determine the metal phase composition. Crystallinity and size were determined using the Scherrer equation. A gas sorption analyzer (GSA, NOVA 1200e) was used to evaluate catalyst texture.

Catalyst acidity was measured via the gravimetric method, with pyridine as a probe molecule [18], and the results were confirmed using Fourier-transform infrared spectroscopy (FTIR, Shimadzu 8201 PC) and  $NH_3$  temperature-programmed desorption ( $NH_3$ -TPD, ChemiSorb 2750 Micromeritics). The  $NH_3$ -TPD instrument ran at  $10^\circ C/min$  between 100 and  $700^\circ C$  and was then held for 10 min at  $700^\circ C$ . Desorbed  $NH_3$  was detected using a thermal conductivity detector (TCD). The peak area was then calculated using standard linear regression in order to determine the catalyst's acidity.

A scanning electron microscope (SEM, JEOL JSM 6510 LA) was used to evaluate the morphology of the catalyst. Each catalyst specimen was prepared using a gold coating. SEM was carried out using the FEI Ltd Inspect-S50. An additional analysis via energy-dispersive X-rays (EDX, EDAX Ltd.) was performed to identify the elemental composition and its location on the catalyst surface.

### Catalyst performance evaluation

The catalytic performance of anisole HDO was studied using a flow reactor (EDULAB). For each test, several grams of catalyst were placed in the reactor and reduced *in situ* in  $H_2$  gas at a rate of 15 mL/min for 2 h. Furthermore, the reactor was heated to  $350^\circ C$  before the anisole flowed at a rate of 10 mL/min with  $H_2$  as a carrier gas. The liquid fraction was obtained after the outflow stream passed through the ice condenser.

The liquid fraction was determined via GC-MS analysis (Shimadzu GCMS-QP2010 SE), while the mass spectra were obtained in the electron ionization (EI) mode and in the  $m/z$  range of 50-600. Peak mass was then identified and quantified according to the Wiley library database.

## Results and discussion

### Copper content

Theoretically, MOR has a larger pore dimension than HZSM-5, resulting in an excellent adsorption capacity. The pore structure of MOR is composed of a 12-membered ring with a dimension of  $6,5 \times 7 \text{ \AA}$  [19], while HZSM-5 is composed of a 10-membered ring with a diameter of  $5-6 \text{ \AA}$  [20]. ANZ, on

the other hand, is primarily made up of a MOR framework. Thus, it appears that its capabilities are somewhat MOR-like. Given that MOR had the greatest adsorption capacity, it is not surprising that the Cu4/MOR catalyst demonstrated the best impregnation efficiency, which was 94% (Table 1).

**Table 1.** Catalyst composition as obtained via XRF

Catalysts	Composition (% w/w)		
	Si	Al	Cu
HZSM-5	51,6	2,67	-
Cu4/HZSM-5	42,4	0,43	2,29
Cu8/HZSM-5	35,5	0,99	4,71
MOR[21]	44,17	0,74	-
Cu4/MOR[21]	39,6	0,64	3,74
Cu8/MOR[21]	36,1	0,6	5,52
ANZ	32,3	3,83	-
Cu4/ANZ	32,9	3,97	3,61
Cu8/ANZ	31,6	3,78	4,58

### Metal phase composition

All the catalysts show diffraction patterns similar to their parent zeolite (Fig. 1). New Cu crystal peaks appear on the catalysts after impregnation. The parent zeolite characteristic peaks remain, indicating that copper impregnation did not harm or change the zeolite structure.

The crystal size is greatly influenced by the catalyst's composition. All catalysts exhibit high crystallinity (up to 96,12%), with varying crystal sizes. The crystal size does not change significantly after impregnation, except for the Cu4/MOR and Cu4/ANZ catalysts.  $Cu(OH)_2$  phases are found in Cu4/MOR catalysts, resulting in large crystal sizes. Meanwhile, the Cu4/ANZ catalyst show the largest crystal size, given the appearance of an unknown crystal at 35, 52, and  $77^\circ$ .

Copper was discovered in a variety of metal phases, including Cu,  $CuO$ ,  $Cu_2O$ , and  $Cu(OH)_2$ . Despite the absence of copper oxide and hydroxide (Fig. 1), the calculation test reveals that they are matched to catalysts. These findings are debatable, but copper oxide and hydroxide may have low intensities in the diffraction pattern of the catalysts. Furthermore, these findings can help to explain the various catalyst colors. Cu/HZSM-5 and Cu/ANZ are dark reddish gray due to their crystal composition. The gray coloration of the catalyst is associated with HZSM-5 and ANZ as the parent zeolite, whereas Cu,  $Cu_2O$ , and  $CuO$  add brown, red, and black to the catalysts, respectively. MOR is a bright white substance, so Cu4/MOR is pale green, which is associated with its  $Cu(OH)_2$  content. Meanwhile, Cu8/MOR is reddish brown due to Cu and  $Cu_2O$ .

The copper metal phase has a distinct diffraction pattern corresponding to ICSD #53246, indicating that the reduction process successfully converted copper ions into copper

metal. The copper crystal peak intensities increase as the copper content increases. The Rietica software with Le bail methods was used to further study the phase composition and the molar percentage of the catalysts (Table 2).

The Cu metal phase was found in all catalysts after impregnation, indicating a successful reduction process.

However, Cu/HZSM-5 and Cu/ANZ contain CuO and Cu<sub>2</sub>O, which indicates that copper was not completely reduced. Cu/MOR appears to be better reduced; here, no CuO was obtained. This work cannot explain the formation of Cu(OH)<sub>2</sub> in Cu4/MOR because copper hydroxide should be easily converted to copper oxide at low temperatures (150 °C) [22].

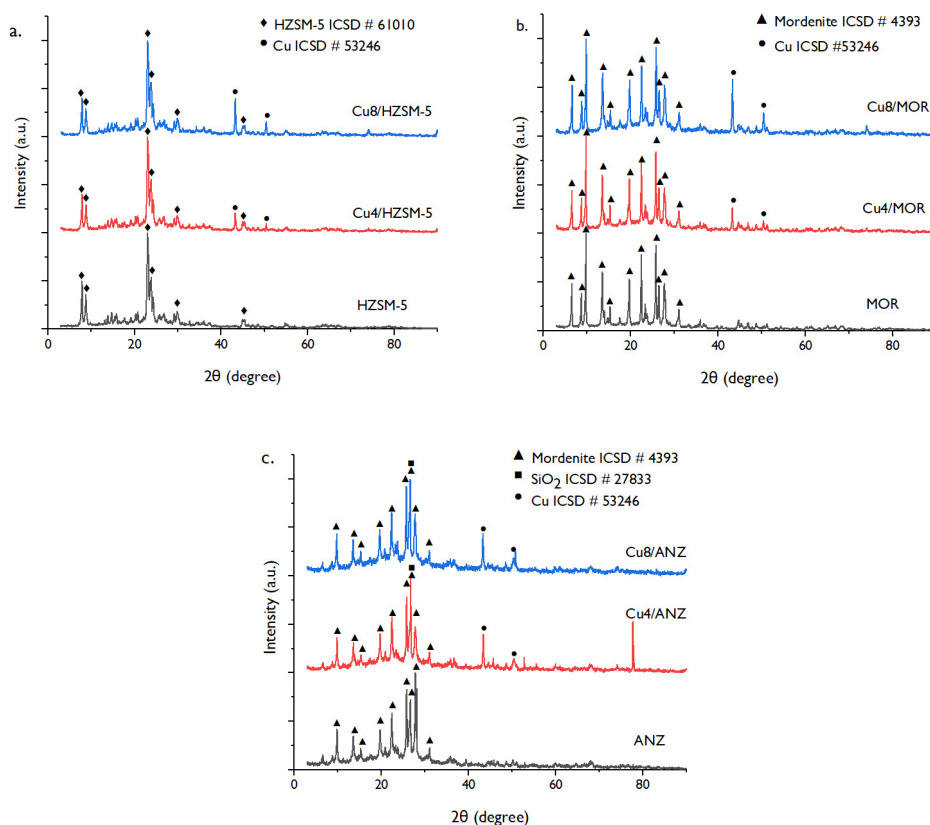


**Figure 1.** X-ray diffraction pattern of the Cu/HZSM-5, Cu/MOR [21], and Cu/ANZ catalysts

**Table 2.** Crystal data for Cu/HZSM-5, Cu/MOR, and Cu/ANZ catalysts based on XRD followed by refinement via the Le Bail method

Catalyst	Crystallinity (%)	Crystal size (nm)	Molar percentage (%)								
			Mordenite #4393	Mordenite #9632	HZSM-5 #61010	Klipnotilolite #66459	SiO <sub>2</sub> #27833	Cu #53246	Cu(OH) <sub>2</sub> #15455	Cu <sub>2</sub> O #53322	CuO #61323
MOR[21]	96,12	35,73	97,91	2,09							
Cu4/MOR[21]	91,99	40,33	97,20	2,07				0,14	0,48	0,11	
Cu8/MOR[21]	92,30	30,32	97,66	2,08				0,14		0,11	
HZSM-5	93,63	24,40			100						
Cu4/HZSM-5	95,42	28,13			89,18			3,18		2,57	5,07
Cu8/HZSM-5	95,52	26,52			89,21			3,16		2,56	5,07
ANZ	90,12	31,15	98,45			1,55					
Cu4/ANZ	95,49	64,18	97,74			1,53	0,25	0,14		0,11	0,23
Cu8/ANZ	94,45	35,70	97,84			1,54	0,25	0,14			0,23



## Textural profile

MOR has the largest surface area and pore volume, as well as the smallest pore size, whereas ANZ has the smallest surface area and pore volume but the largest pore size despite its high structural similarity to MOR (Table 3). The fact that ANZ has a significantly lower Si/Al ratio than MOR, which impacts the surface area and pore profile, may help to explain this discrepancy. HZSM-5 had a middling surface area, pore volume, and pore size when compared to MOR and ANZ.

**Table 3.** Surface area and pore profile of catalysts based on  $N_2$  isotherms

Catalyst	$S_{\text{Internal}}^a$ ( $m^2/g$ )	$S_{\text{BET}}^b$ ( $m^2/g$ )	$V_p^c$ ( $cc/g$ )	Pore size <sup>c</sup> (nm)
HZSM-5	207,1	319,1	0,29	163,3
Cu4/HZSM-5	151,4	304,3	0,26	180,2
Cu8/HZSM-5	141,2	299,2	0,26	181,7
MOR	362,5	506,1	0,33	136,8
Cu4/MOR	244,6	406,0	0,34	173,0
Cu8/MOR	205,1	461,9	0,42	186,9
ANZ	90,5	182,0	0,17	201,5
Cu4/ANZ	77,9	190,7	0,20	224,6
Cu8/ANZ	68,8	207,2	0,19	193,6

<sup>a</sup> Internal surface area calculated using T-plots

<sup>b</sup> BET surface area estimated with relative pressure in the 0,05-0,3 range

<sup>c</sup> Total pore volume and mean pore radius calculated using the BJH model

Typically, copper bonds to the surface of the zeolite pores and blocks them, reducing the surface area and pore volume. This is consistent with the catalysts' internal pores, which progressively close up after impregnation. These findings also suggest that copper was successfully attached to the cavity of zeolites by impregnation. Copper does not wholly block the zeolite's pores, which is beneficial for catalytic reactions.

After impregnation, the surface area of Cu/HZSM-5 catalysts slightly decreases, while that of Cu/ANZ increases. Meanwhile, copper impregnation reduces the surface area of MOR, but Cu8/MOR catalysts have a larger surface area than Cu4/MOR catalysts. These results are confusing but may be clarified by considering the catalysts' increase in external surface area and total pore volume. The zeolite's pores are limited, and some copper prefers to stick to the external surface of the zeolite. Subsequently, copper accumulates and entails roughness, which causes a slight increase in the surface area. Moreover, copper is attached to the pore mouth, thus extending the porosity and slightly increasing the pore volume. Therefore, catalysts exhibit a large surface area after being impregnated with 8% (w/w) rather than 4% (w/w) due to the excess copper on the external surface of the zeolites.

The pore size distribution of the catalysts was evaluated using the BJH method at a 1,5-100 nm radius (Fig. 2). The distribution peaks were found to be broad, which means

that the catalysts have various pore sizes. It also suggests that the pores are more slit-shaped than cylindrical.

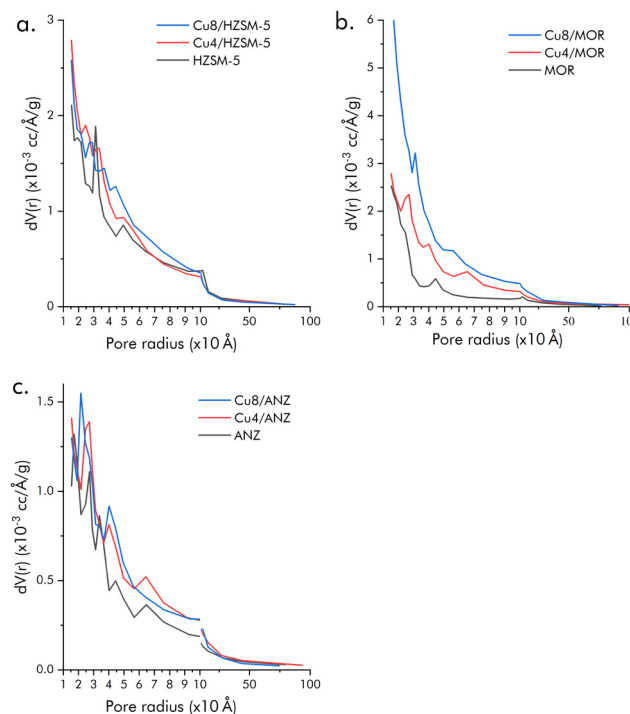


**Figure 2.** Pore distribution of Cu/HZSM-5, Cu/MOR, and Cu/ANZ catalysts

## Functional group and acidity

The FTIR spectra show peaks at 1 200-450  $cm^{-1}$ , which is typical of zeolites. The external T-O (T = tetrahedral Si or Al) exhibits symmetric stretching vibrations at around 1 200 and 1 050  $cm^{-1}$ , as well as asymmetric stretching at around 820 and 790  $cm^{-1}$  (Fig. 3). Meanwhile, the peaks at around 650 and 450  $cm^{-1}$  are attributed to internal T-O symmetric and asymmetric stretching, respectively. The T-O groups appear to be dominant, which indicates that zeolite structure is the main component of the catalysts. However, the T-O vibration pattern seems different for HZSM-5, MOR, and ANZ, due to their different structure and Si/Al ratio. Copper impregnation did not significantly change the T-O functional group, which indicates that the zeolite structure is not ruined by copper, which agrees with XRD results.

The O-H groups are represented by the broad peak of OH stretching at around 3 300-3 600  $cm^{-1}$  and OH bending at around 1 600  $cm^{-1}$ . The O-H group is associated with water molecules or the Bronsted acid site of catalysts. HZSM-5 showed the most significant peak area in the O-H group, indicating that it had the most acidic nature when compared to MOR and ANZ. Furthermore, copper impregnation slightly decreased the peak area of the OH group on the catalysts due to cation exchange. However, acidity evaluation needs further confirmation using more reliable techniques.

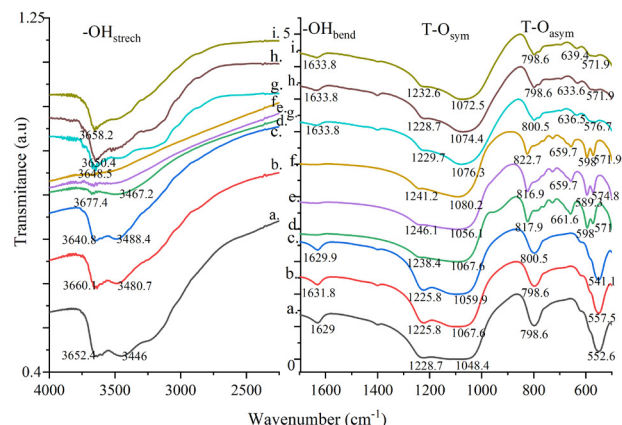


**Figure 3.** FTIR spectra of a) HZSM-5, b) Cu4/HZSM-5, c) Cu8/HZSM-5, d) MOR, e) Cu4/MOR, f) Cu8/MOR, g) ANZ, h) Cu4/ANZ, and i) Cu8/ANZ

Catalyst acidity was evaluated using pyridine and ammonia as probe molecules (Table 4). Pyridine gravimetry only determines the total acidity, whereas  $\text{NH}_3$ -TPD can distinguish the acid strength of several sites on the catalysts. All catalysts showed more than one desorption peak in the  $\text{NH}_3$ -TPD test, indicating several acid sites with different strengths.

**Table 4.** Acidity of Cu/HZSM-5, Cu/MOR, and Cu/ANZ catalysts based on  $\text{NH}_3$ -TPD and pyridine gravimetry

Catalyst	TPD (mmol/g) <sup>1</sup>				Gravimetry (mmol/g) <sup>2</sup>
	Weak	Medium	Strong	Total	
HZSM-5	0,75	0,68	0,14	1,56	0,85
Cu4/HZSM-5	0,64	0,28	0,43	1,36	0,69
Cu8/HZSM-5	0,52	0,20	0,57	1,28	0,66
MOR	0,19	0,10	0,39	0,68	0,89
Cu4/MOR	0,05	0,29	0,14	0,49	0,59
Cu8/MOR	0,00	0,11	0,23	0,34	0,50
ANZ	0,75	0,00	0,92	1,67	1,08
Cu4/ANZ	0,85	0,00	1,09	1,94	1,23
Cu8/ANZ	0,12	0,00	0,23	0,35	0,94

<sup>1</sup>TPD acidity was calculated based on the area of ammonia desorption peak and a standard linear regression

<sup>2</sup>Gravimetric acidity was calculated based on the difference in weight of the catalyst after pyridine adsorption

The acidity of the catalysts decreased after copper impregnation, except for Cu4/ANZ. [23] reported that impregnation with 0-3% (w/w) increased the acidity of the catalyst by adding Bronsted acid sites. Meanwhile, another report revealed that the catalyst acidity decreased by 5-30% (w/w) with copper impregnation due to pore blockage by excess Cu [8]. Pore blockage was also observed in this work, as seen in the decrease in micropore area (Table 3). However, Cu4/ANZ exhibited the most remarkable mean pore size, thus preventing pore blockage.

## Morphology and mapping elements

Copper impregnation did not change the morphology of the catalysts. Meanwhile, small spherical particles (*i.e.*, copper particles) were found on the catalyst after impregnation. These copper particles are shiny and more clearly observed at a scale of 1  $\mu\text{m}$ , as depicted in the inset image of Fig. 4. The number of copper particles was higher after copper impregnation at 8% (w/w) in comparison with that at 4% (w/w), which agrees with XRF results. Furthermore, the particles appear to be evenly distributed on the catalysts, indicating a good dispersion of copper.

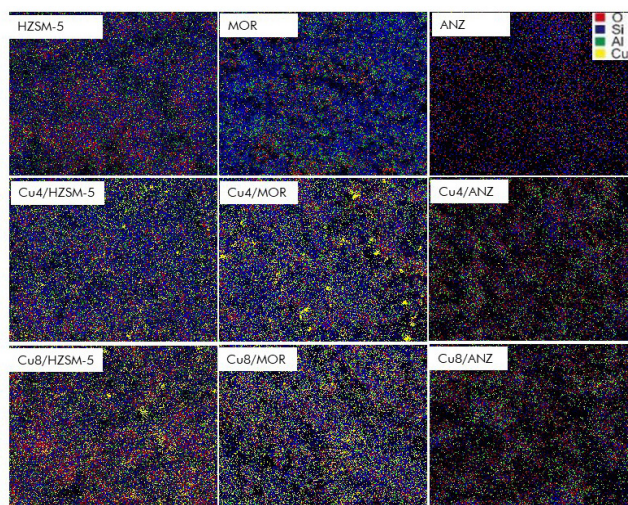
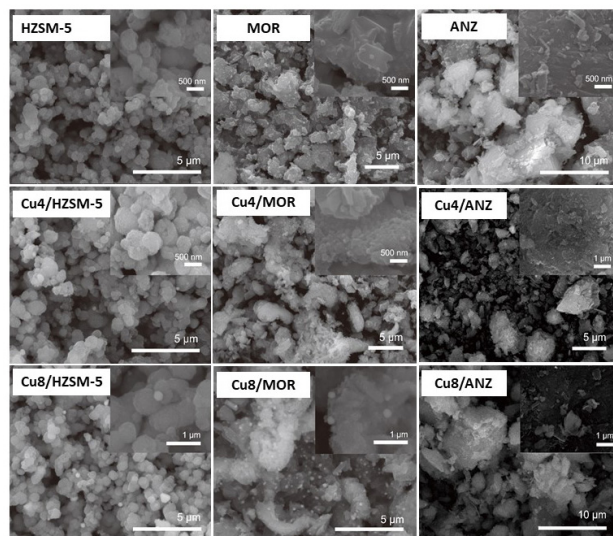


**Figure 4.** SEM image and mapping elements of the Cu/HZSM-5, Cu/MOR, and Cu/ANZ catalysts

## Anisole hydrodeoxygenation

HZSM-5, MOR, and ANZ exhibited a higher conversion of anisole than the thermal reaction, indicating that the support can provide a catalytic effect, even without adding metals (Table 5). Zeolites have acid sites that can dissociate  $\text{H}_2$  or absorb oxygenated compounds. Conversely, oxygen



electrons can interact with the unsaturated orbitals of Lewis acid sites [5].

The conversion for anisole HDO is  $\text{HZSM-5} > \text{MOR} > \text{ANZ}$ . Zeolites have different acidity and surface area, so they significantly affect HDO catalytic activity [8]. Higher catalyst acidity and surface area lead to higher HDO activity [8], [23]. The large surface area is an ideal adsorption site for reactants before they are activated and converted to products. Meanwhile, the acidity of the zeolite serves to dissociate  $\text{H}_2$  or bind to the anisole's oxygen groups. The Bronsted acid site interacts with the oxygen atom because the  $\pi$ -electrons of the oxygen are more electronegative than the  $\pi$ -electrons of the aromatic ring [24]. On the other hand, the Lewis acid site can also adsorb oxygen atoms from the anisole through electron vacancy [5].

The HZSM-5 catalyst has the highest acidity and a large surface area, thus providing the best anisole HDO catalytic activity. HZSM-5 showed the highest conversion (41,09%) and the highest liquid yield (18,11%), as shown in Table 5. This excellent performance is probably due to its high surface area and acidity. The BTX product was successfully obtained from the anisole HDO reaction. The ANZ catalyst, on the other hand, has the lowest surface area, so it has poor catalytic activity. The results also demonstrated that the catalyst performed better as a powder than as a pellet in terms of anisole conversion and liquid products yield. The catalyst has a higher surface area in powder form, resulting in a better catalyst-anisole contact.

**Table 5.** Product of anisole HDO regarding the Cu/MOR, Cu/HZSM-5, and Cu/ANZ catalysts at 350 °C

Catalyst	Conversion (%) <sup>b</sup>	Liquid product (mmol/g) <sup>b</sup>				
		Yield (%) <sup>b</sup>			Selectivity (%)	
		Total	BTX <sup>c</sup>	Phs <sup>d</sup>	BTX <sup>c</sup>	Phs <sup>d</sup>
Thermal	10,31	0,68	0,37	0,14	53,95	21,05
HZSM-5 <sup>a</sup>	36,55	12,00	0,51	6,37	4,28	53,12
HZSM-5	41,09	18,11	1,33	11,11	7,31	60,94
Cu4/HZSM-5	20,91	7,62	0,26	6,04	3,41	79,29
Cu8/HZSM-5	31,47	12,23	0,65	9,53	5,34	77,84
MOR	29,85	7,02	0,06	4,55	0,88	64,84
Cu4/MOR	8,04	4,96	0,11	3,07	2,15	61,91
Cu8/MOR	20,61	5,06	0,04	3,02	0,83	59,67
ANZ	23,77	3,23	0,03	2,45	0,98	75,68
Cu4/ANZ	21,17	4,32	0,05	3,26	1,15	75,38
Cu8/ANZ	24,43	1,60	0,000	1,25	0,00	78,26

<sup>a</sup>HZSM-5 catalyst in pellet form

<sup>b</sup>Calculated as weight percentage of reactant mass

<sup>c</sup>BTX

<sup>d</sup>Phs: phenolic compounds

According to [4], adding copper metal reduces anisole HDO conversion for HZSM-5, MOR, and ANZ. The loss of some zeolite acid sites due to metal loading indicates that it causes decreased catalytic activity. The metal is also believed to be less active at reaction temperatures below 400 °C. In addition, Cu loading also reduces the surface

area of the HZSM-5, MOR, and ANZ micropores, which decreases the catalytic activity of anisole HDO [8], [23]. Nevertheless, due to the synergy effect between metal and zeolite, the Cu8/zeolite catalyst showed better conversion than Cu4/zeolite. The unique performance of the Cu4/MOR catalyst is thought to be due to the catalyst's metallic  $\text{Cu}(\text{OH})_2$  phase.

Coke is undesirable in HDO anisole reactions because it can deactivate the catalyst. However, it was discovered that, as the pore size of the catalyst decreased, the coke increased. The HZSM-5 catalyst produces the most coke due to its small pore size (136,8 nm). Metal additions to HZSM-5 and MOR increased the pore size of the catalyst, resulting in coke reduction. However, because the pore size was too large, the presence of metals did not affect coke formation in the Cu/ANZ catalyst. A certain amount of coke produced as a byproduct can clog the pores of the catalyst, rendering it inactive. As a result, the catalyst's large pore size is advantageous because it prevents coke formation and deactivation. On the other hand, too large a pore size can also have a harmful effect, as zeolites can lose their pore selectivity.

The total yield of the liquid product from the HDO anisole reaction using Cu/HZSM-5, Cu/MOR, and Cu/ANZ is presented in Fig. 5. Phenol and methyl anisole were the dominant liquid products obtained from HDO anisole. Based on kinetics studies, the anisole-HDO reaction occurred as a bimolecular reaction with a short contact time and high reactant concentrations [25]. The bimolecular reaction produced phenol and methyl anisole by combining two anisole compounds.

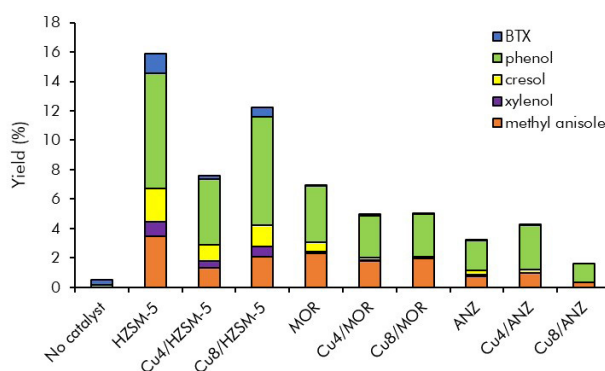


**Figure 5.** Liquid yield product of anisole HDO using the Cu/HZSM-5, Cu/MOR, and Cu/ANZ catalysts

Phenol (Phs) corresponds to each catalyst's main product of anisole HDO. The presence of phenolic products follows the theory that the anisole HDO reaction consists of two or more steps. One step is the transmethylation reaction between two anisoles, where the methoxy bond ( $-\text{O}-\text{CH}_3$ ) from one anisole is hydrogenated and broken to produce Phs and methyl. The methyl group ( $-\text{CH}_3$ ) is then bonded back to the phenol to produce methyl Phs. In addition, transmethylation reactions can also occur when the methyl group is released

in the first step and reacts with another anisole, producing methyl anisole. The second bimolecular reaction produces cresol and xylenol with longer contact times. However, in this study, the contact time was less than one hour, so there was Phs dominance over cresol and xylenol.

The Cu/zeolite catalyst increased the Phs yield from 8 to 55 times compared to the thermal reaction. Except for MOR, the addition of Cu metal to zeolite increases the yield due to the synergistic effect. Copper metal plays a role in absorbing and separating hydrogen [26], and the dissociated hydrogen interacts with the methoxy group through spillover hydrogen, resulting in a hydrogenation reaction [24]. At the same time, zeolite provides Bronsted acid sites (Fig. 6).

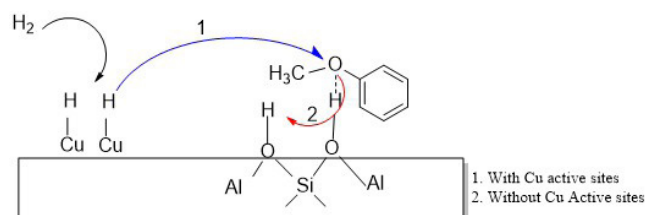


**Figure 6.** Proposed mechanism for the interaction of zeolite-embedded Cu catalysts with anisole in the modified HDO reaction [24]

BTX products indicate a successful anisole HDO reaction. BTX can be formed through one- and two-step deoxygenation routes [1]. Acidic catalysts, such as zeolites, have a tendency towards a two-step anisole HDO reaction [5]. This route was also found in this study, where BTX was the final product.

The maximum yield of the BTX product was 1,33% (w/w), which indicated that the HDO anisole reaction had not been completed. Contact time, bond energy, and metal activity can cause an unsuitable reaction. The short contact time caused the trans-alkylation reaction to dominate, and deoxygenation, the second step, did not occur. Meanwhile, the bond energy of RO-R (339 kJ/mol) was lower than that of Ar-OH (468 kJ/mol) [25]. Thereupon, anisole is more easily converted to phenol instead of forming benzene. Furthermore, metal-zeolite synergism is important in anisole HDO reactions such as transmethylation [27]. Unfortunately, metal activity is low at temperatures below 400 °C [28], so there is no BTX yield decrease caused by the synergy effect.

The effect of temperature on the catalyst activity was examined, finding that the conversion increased significantly (Table 6). The high temperature can provide a lot of energy, which allows the methoxy anisole groups to break and react with hydrogen to form BTX products easily.

At 500 °C, although HZSM-5 provided a higher liquid product yield and conversion, the Cu8/HZSM-5 catalyst produced the highest BTX yield and selectivity. This finding supports the notion that high temperatures are required for Cu metal to synergize with zeolite and increase BTX activity and selectivity.

**Table 6.** Effect of temperature at anisole HDO for the HZSM-5 and Cu8/HZSM-5 catalysts

Catalyst	Temperature (°C)	Conversion (%) <sup>1</sup>	Liquid product (mmol/g) <sup>2</sup>			
			Yield (%) <sup>a</sup>		Selectivity (%)	
			BTX <sup>b</sup>	Phs <sup>c</sup>	BTX <sup>b</sup>	Phs <sup>c</sup>
HZSM-5	350	41,09	1,33	11,11	7,31	60,94
HZSM-5	500	61,87	12,15	16,38	37,55	50,62
Cu8/HZSM-5	350	31,47	0,65	9,53	5,34	77,84
Cu8/HZSM-5	500	53,28	13,06	14,79	42,45	48,05

<sup>a</sup>Calculated as the weight percentage of reactant mass

<sup>b</sup>BTX: benzene, toluene, and xylene

<sup>c</sup>Phs: phenolic compounds

## Conclusion

This study was dedicated to the modification of copper attachment on HZSM-5, MOR, and ANZ, obtaining the best impregnation efficiency (94%), which corresponded to Cu4/MOR. The structures of HZSM-5, MOR, and ANZ were not damaged after impregnation with copper, which was confirmed via structural analysis using XRD and FTIR. Further analysis revealed copper as a metal phase of Cu, Cu<sub>2</sub>O, CuO, and Cu(OH)<sub>2</sub>. Copper impregnation affects the surface area and pore volume of the parent zeolite. The internal surface area and micropore volume of the zeolite continued to decrease after impregnation, indicating that the copper adhered to the pores of the zeolite. This was supported by total acidity reduction data.

However, some copper particles adhered to the zeolite's outer surface, causing roughness and slightly increasing the BET surface area. Due to its high surface area and acidity, HZSM-5 provided the best anisole HDO conversion and BTX selectivity. At 350 °C, the contribution of Cu metal as the active site was less pronounced. However, Cu was more active at 500 °C, which significantly increased anisole HDO conversion (53,28%) and BTX selectivity (42,45%).

## Acknowledgements

The project presented in this article was supported by SEBELAS MARET University under HIBAH MANDATORY (2021), with grant number 260/UN27.22/HK.07.00/2021.

## CRedit author statement

All authors have participated in a) conception and design or data analysis and interpretation; (b) drafting the article or revising it critically for important intellectual content; and (c) approving of the final version of the manuscript.

N. K. D.: conceptualization and supervision; N. K. D., H. Y.: writing – review and editing; H. E., R. F., N. I. F.: formal analysis; S. A. I.: investigation.



## Conflicts of interest

The authors confirm that this work is original and has not been published elsewhere nor is it currently under consideration for publication elsewhere. The authors declare that they have no conflict of interest.

## Data availability

The datasets generated and/or analyzed during the current study are available from the corresponding author upon reasonable request.

## References

- [1] A. R. K. K. Gollakota, M. Reddy, M. D. Subramanyam, and N. Kishore, "A review on the upgradation techniques of pyrolysis oil," *Renew. Sustain. Energy Rev.*, vol. 58, pp. 1543-1568, 2016, <https://doi.org/10.1016/j.rser.2015.12.180>
- [2] X. Li *et al.*, "Heterogeneous sulfur-free hydrodeoxygenation catalysts for selectively upgrading the renewable bio-oils to second generation biofuels," *Renew. Sustain. Energy Rev.*, vol. 82, pp. 3762-3797, 2018, <https://doi.org/10.1016/j.rser.2017.10.091>
- [3] X. Wang, B. Du, L. Pu, Y. Guo, H. Li, and J. Zhou, "Effect of particle size of HZSM-5 zeolite on the catalytic depolymerization of organosolv lignin to phenols," *J. Anal. Appl. Pyrolysis*, vol. 129, pp. 13-20, Jan. 2018, <https://doi.org/10.1016/j.jaap.2017.12.011>
- [4] J. Zhang, B. Fidalgo, A. Kolios, D. Shen, and S. Gu, "Mechanism of deoxygenation in anisole decomposition over single-metal loaded HZSM-5: Experimental study," *Chem. Eng. J.*, vol. 336, pp. 211-222, Mar. 2018, <https://doi.org/10.1016/j.cej.2017.11.128>
- [5] K. A. Rogers and Y. Zheng, "Selective deoxygenation of biomass-derived bio-oils within hydrogen-modest environments: A review and new insights," *ChemSusChem*, vol. 9, no. 14, pp. 1750-1772, 2016, <https://doi.org/10.1002/cssc.201600144>
- [6] S. Popov and S. Kumar, "Rapid hydrothermal deoxygenation of oleic acid over activated carbon in a continuous flow process," *Energy and Fuels*, vol. 29, no. 5, pp. 3377-3384, 2015, <https://doi.org/10.1021/acs.energyfuels.5b00308>
- [7] J. Zhang, B. Fidalgo, S. Wagland, D. Shen, X. Zhang, and S. Gu, "Deoxygenation in anisole decomposition over bimetallic catalysts supported on HZSM-5," *Fuel*, vol. 238, pp. 257-266, Feb. 2019, <https://doi.org/10.1016/j.fuel.2018.10.129>
- [8] C. Li *et al.*, "Catalytic cracking of Swida wilsoniana oil for hydrocarbon biofuel over Cu-modified ZSM-5 zeolite," *Fuel*, vol. 218, no. January, pp. 59-66, Apr. 2018, <https://doi.org/10.1016/j.fuel.2018.01.026>
- [9] E. Roduner, "Understanding catalysis," *Chem. Soc. Rev.*, vol. 43, no. 24, pp. 8226-8239, 2014, <https://doi.org/10.1039/C4CS00210E>
- [10] R. Lippi *et al.*, "Unveiling the structural transitions during activation of a CO<sub>2</sub> methanation catalyst RuO/ZrO<sub>2</sub> synthesised from a MOF precursor," *Catal. Today*, vol. 368, pp. 66-77, May 2021, <https://doi.org/10.1016/j.cattod.2020.04.043>
- [11] J. Zhang, B. Fidalgo, A. Kolios, D. Shen, and S. Gu, "The mechanism of transmethylation in anisole decomposition over Brønsted acid sites: Density functional theory (DFT) study," *Sustain. Energy Fuels*, vol. 1, no. 8, pp. 1788-1794, 2017, <https://doi.org/10.1039/C7SE00280G>
- [12] Y. Zheng *et al.*, "Efficient and stable Ni-Cu catalysts for ex situ catalytic pyrolysis vapor upgrading of oleic acid into hydrocarbon: Effect of catalyst support, process parameters and Ni-to-Cu mixed ratio," *Renew. Energy*, vol. 154, pp. 797-812, Jul. 2020, <https://doi.org/10.1016/j.renene.2020.03.058>
- [13] Q. Che, W. Yi, Y. Liu, X. Wang, H. Yang, and H. Chen, "Effect of mesopores in ZSM-5 on the catalytic conversion of acetic acid, furfural, and guaiacol," *Energy and Fuels*, vol. 35, no. 7, pp. 6022-6029, 2021, <https://doi.org/10.1021/acs.energyfuels.0c04415>
- [14] G. M. H. A. Ihsan, K. D. Nugrahaningtyas, D. M. Widjonarko, and F. Rahmawati, "Structure and morphology of the (Ni, Co) Mo/Indonesian natural zeolite," *IOP Conf. Ser. Mater. Sci. Eng.*, vol. 578, art. 012009, 2019, <https://doi.org/10.1088/1757-899X/578/1/012009>
- [15] K. D. Nugrahaningtyas, R. S. R. Suharbiansah, W. W. Les-tari, and F. Rahmawati, "Metal phase, electron density, textural properties, and catalytic activity of CoMo based catalyst applied in hydrodeoxygenation of oleic acid," *Evergreen*, vol. 9, no. 2, pp. 283-291, Apr. 2022, <https://doi.org/10.5109/4793665>
- [16] K. D. Nugrahaningtyas, M. M. Putri, and T. E. Saraswati, "Metal phase and electron density of transition metal/HZSM-5," *AIP Conf. Proc.*, vol. 2237, art. 020003, 2020, <https://doi.org/10.1063/5.0005561>
- [17] K. D. Nugrahaningtyas, M. F. Kurniawati, A. Masykur, N. 'Abidah Quratul'aini, and N. 'Abidah Quratul'aini, "Periodic trends in the character of first-row transition metals-based catalysts embedded on mordenite," *Moroccan J. Chem.*, vol. 10, no. 3, pp. 375-386, May 2022, <https://revues.imist.ma/index.php/morjchem/article/view/32665/16923>
- [18] T. Barzetti, E. Selli, D. Moscotti, and L. Forni, "Pyridine and ammonia as probes for FTIR analysis of solid acid catalysts," *J. Chem. Soc. - Faraday Trans.*, vol. 92, no. 8, pp. 1401-1407, 1996, <https://doi.org/10.1039/ft9969201401>
- [19] M. A. Klunk *et al.*, "Synthesis and characterization of mordenite zeolite from metakaolin and rice husk ash as a source of aluminium and silicon," *Chem. Pap.*, vol. 74, pp. 2481-2489, 2020, <https://doi.org/10.1007/s11696-020-01095-4>
- [20] A. S. Al-Dughaiter, H. De Lasa, and H. De Lasa, "HZSM-5 zeolites with different SiO<sub>2</sub> Al<sub>2</sub>O<sub>3</sub> ratios. Characterization and NH<sub>3</sub> desorption kinetics," *Ind. Eng. Chem. Res.*, vol. 53, no. 40, pp. 15303-15316, Oct. 2014, <https://doi.org/10.1021/ie4039532>
- [21] A. I. Sabilagusti, K. D. Nugrahaningtyas, and Y. Hidayat, "Synthesis and metal phases characterization of mordenite supported copper catalysts," *J. Phys. Conf. Ser.*, vol. 1912, art. 012032, 2021, <https://doi.org/10.1088/1742-6596/1912/1/012032>

- [22] Y. Cudennec and A. Lecerf, "The transformation of  $\text{Cu}(\text{OH})_2$  into  $\text{CuO}$ , revisited," *Solid State Sci.*, vol. 5, no. 11-12, pp. 1471-1474, 2003, <https://doi.org/10.1016/j.solidstatesciences.2003.09.009>
- [23] W. B. Widayatno et al., "Upgrading of bio-oil from biomass pyrolysis over Cu-modified  $\beta$ -zeolite catalyst with high selectivity and stability," *Appl. Catal. B Environ.*, vol. 186, pp. 166-172, 2016, <https://doi.org/10.1016/j.apcatb.2016.01.006>
- [24] Z. He and X. Wang, "Hydrodeoxygenation of model compounds and catalytic systems for pyrolysis bio-oils upgrading," *Catal. Sustain. Energy, Versita*, vol. 1, no. 2013, pp. 28-52, Oct. 2012, <https://doi.org/10.2478/cse-2012-0004>
- [25] X. Zhu, R. G. Mallinson, and D. E. Resasco, "Role of transalkylation reactions in the conversion of anisole over HZSM-5," *Appl. Catal. A Gen.*, vol. 379, no. 1-2, pp. 172-181, May 2010, <https://doi.org/10.1016/j.apcata.2010.03.018>
- [26] J. Albo, M. Perfecto-Irigaray, G. Beobide, and A. Irabien, "Cu/Bi metal-organic framework-based systems for an enhanced electrochemical transformation of  $\text{CO}_2$  to alcohols," *J. CO<sub>2</sub> Util.*, vol. 33, pp. 157-165, 2019, <https://doi.org/10.1016/j.jcou.2019.05.025>
- [27] X. Zhu, L. L. Lobban, R. G. Mallinson, and D. E. Resasco, "Bifunctional transalkylation and hydrodeoxygenation of anisole over a Pt/HBeta catalyst," *J. Catal.*, vol. 281, no. 1, pp. 21-29, 2011, <https://doi.org/10.1016/j.jcat.2011.03.030>
- [28] J. Zhang, B. Fidalgo, S. Wagland, D. Shen, X. Zhang, and S. Gu, "Deoxygenation in anisole decomposition over bimetallic catalysts supported on HZSM-5," *Fuel*, vol. 238, pp. 257-266, 2019, <https://doi.org/10.1016/j.fuel.2018.10.129>